A Study on the positioning accuracy based on different VOI selection of ExacTrac x-ray System

li-rong zhao
Xinqiao Hospital
Jin-Dong Qian
Xinqiao Hospital
yibing zhou
Xinqiao Hospital
Jian-Guo Sun (sunjg09@aliyun.com)
Xinqiao Hospital

Article

Keywords: volume of interest (VOI), cranial phantom, positioning accuracy, ExacTrac system

Posted Date: April 18th, 2022

DOI: https://doi.org/10.21203/rs.3.rs-1548273/v1

Abstract

This study aimed to compare the different volume of interest (VOI) selection among the VOI of Head & Neck (HN), VOI of Head only (H), and VOI of Neck (N) only when used for cranial phantom with the imaging guidance system ExacTrac. Exactrac cranial anthropomorphic phantoms was positioned with known set-up deviations from the reference position in the linear accelerator. Verification accuracy was evaluated based on the residual root-mean-square (RMS) positioning error after image registration based on different volume of interest (VOI) selection. The RMS in the translational dimensions was < 0.6 mm for online matching and < 1.1 mm for VOI of Head & Neck (HN) and VOI of Head only (H) offline matching. For VOI of Neck only(N), the RMS in the translational dimensions with was < 0.8 mm. Furthermore, the RMS in the rotational dimensions was < 0.2° for VOI of Head & Neck (HN) and < 0.3° for VOI of Head only (H) offline matching. For VOI of Neck only (N), the RMS in the rotational dimensions was < 0.4°. The minimum setup errors were observed when VOI Head & Neck (HN) was selected. For 75 neck patients, the RMS were statistical significant ($p < 0.05$) in the longitudinal and vertical translational directions. For 75 head&neck cancer patients, the RMS of differences in vertical translational direction and pitch and yaw rotational directions with different selection of VOIs (PTV only and H&N) were statistical significant ($p < 0.05$). It was concluded that image registration method using larger VOI is helpful to improve the registration accuracy.

Introduction

Nasopharyngeal cancer (NPC) is the most common head and neck cancer in southern China [1–3]. Recent technical developments in planning and delivering intensity-modulated radiation therapy (IMRT) offer extraordinary ways for producing intricately shaped radiation doses that closely conform to the tumor dimensions while sparing sensitive structures [4–6]. The advance of IMRT sets more strict requirements on beam targeting accuracy. It is challenging to location patients exactly using tattooing or skin markings, especially for patients with moveable skin. Therefore, image guidance is indispensable in radiotherapy to correct interfractional setup error in order to guarantee correct dose delivery. CBCT provides highresolution 3D information of the patients in the treatment position and thus has great potential for correct target localization and irradiation dose verification [7, 8]. However, in fact, its applications are limited by some practical facts containing relatively long image acquisition time, relatively high imaging dose, high nonmedical insure charge, and uncomfortable for patients due to long scanning time. Because of a limited view of projections, the ExacTrac cannot provide as much information as CBCT [9, 10]. Yet, the ExacTrac could provide other clinical benefits involving quicker patient position using the 6D robic couch, quicker image acquisition time, the ability to monitor patient motion during treatment, and a relatively low radiation dose to the patient [11–13]. Our recently study demonstrated that no statistically significant difference was shown in patient alignment between weekly 3D CBCT and 2D kV imaging [14]. The relative research has found that the usage of daily image guidance with ExacTrac 6D imageguided system is an effective method to imcrease the accuracy of headandneck patients. In all, the ExacTrac X-ray images obtaining and registering to DRRs (digitally reconstructed radiographs) can use bony-anatomy matching

to estimate 6D translational and rotational shifts. Image fusion algorithms are mostly based on bone anatomy and by moving the treatment couch to a position the shifts are calculated and applied that matches anatomically with the reference images. It is difficult for the treating physician to anticipate how the region for registration will influence the final tumour and organ alignment. For clinical patients studies, there are too many complicated factors when we attempt to research the contributing factors of the VOI selection on set-up errors such as inter-fraction PTV movement due to head and neck position and inter-fraction setup error, even though a custom immobilization device is fit to each patient before the planning CT scan is performed. The custom mask system does not place the head at the exact same position every fraction because it allows for a small degree of motion due to shifting of skin and facial tissues. The advantage of using phantom in the present study was that a known range of set-up deviations could be marked on the phantoms for repeated measurements, which would not be possible in patients. The underlying uncertainties of the phantom study can guide understanding of the fundamental limitations of IGRT in an ideal patient. Hence in my paper, registration accuracy was examined by Extrac cranial verification phantom with varying VOI and to assess whether VOI affects automatic image registration for clinical settings.

Methods And Materials

Phantom data

Exactrac Cranial Verification Phantom (Radiology Support Devices Inc., Long Beach, CA) with three 5mm /0.2 inch diameter tungsten carbide spheres was used in the investigation. It was made tissue equivalent material embedded with natural human skeleton, which provided adequate bony definitions for matching. The cranial phantom was scanned by the computed tomography-simulator unit (Brilliance CT, Philips, Cleveland, USA) in supine position following the local departmental scanning protocols of the 2 regions, respectively. A dummy plan was created for each phantom by the Eclipse treatment planning system (Version 15.6; Varian Medical Systems, Palo Alto, USA), and DRRs of the required projections centered at the isocenter were generated. The CT images of the phantom were transferred from Varian Eclipse (Version 15.6; Varian Medical Systems, Palo Alto, USA) work station to ExacTrac system and which were used as reference images in the image registrations. In the treatment unit, the phantom was immobilized with MedTech frame on the treatment couch. Marks at the reference position, which included the anterior midline, the reference principal plane, and 2 lateral horizontal levels, were drawn on the phantoms with the help of the laser system. The cranial phantom was immobilized in the same state for both the verification image using 6D ExacTrac online and offline. In addition, after radiation treatment, registration between the computed tomography simulation images and the ExacTrac images was performed with offline 6D fusion in an offline review. The phantoms were then moved to the assigned deviations with known magnitudes from the reference marks in 3 directions, namely, the lateral translation (x-direction: ± 1, ± 2, ± 3, ± 5 and ± 10 mm), the longitudinal translation (y-direction: ± 1, ± 2, ± 3, ± 5 and ± 10 mm) and the vertical translation (z-direction: ± 1, ± 2, ± 3, ± 5 and ± 10 mm) and marks were made at each deviation accordingly (Figs. 2). After the phantom was moved to isocenter with the ExacTrac 6D couch, 2

orthogonal ExacTrac X-ray images were taken. The phantom was then shifted using the 6D couch according to the image registration results. The study was conducted for each of the 40 isocenters.

Patient data

A total of 2320 daily ExacTracs of 225 patients were analyzed. Of the total 225 patients, 75 were head and neck cancer patients, 75 were only neck cancer patients and the other 75 were the cranial cancer patients. All patients were fixed in treatment position with MedTech frame and individualized thermoplastic facial masks. All underwent virtual CT simulation with 3.0 mm slices following the local departmental scanning protocols of the 2 regions, respectively. Magnetic resonance imaging (MRI) scans were also obtained accordingly. The CT and MRI fusion images were transferred to Varian Eclipse (Version 15.6; Varian Medical Systems, Palo Alto, USA) work station to create IMRT or ARC plans. Written informed consent was obtained from all patients and the study was approved by the Medical Ethics Committee of Xinqiao Hospital, Army Military Medical University. In addition, the reporting in the research follows the recommendations in the ARRIVE guidelines. For 75 cranial cancer patients, the VOI was designed for the whole CT range or head only. For 75 neck cancer patients, the VOI was designed for the whole CT range or neck only. For 75 head&neck cancer patients, the VOI was designed for the whole CT range or head only.

In both phantom and patient studies, 6D offline image registrations with different VOIs were performed and residual errors in the 3 translational directions (vertical, longitudinal, and lateral) and in the 3 rotational directions (rotation, pitch, and roll) were evaluated.

Calibration of IGRT System

A routine Winston-Lutz test is performed to verify radiation-laser isocenter coincidence at first. Before daily use, the ExacTrac IR system is calibrated using the room lasers to define the IR isocenter. The infrared camera calibration is accomplished according to ExacTrac Clinical Users Guide version 5.0 using the infrared calibration grid, which is a frame comprised of 25 infrared markers at known relative locations from one another. Then, the position of isocenter in the ExacTrac IR system is registered using the isocenter phantom. Finally, the X-ray calibration phantom is aligned to IR isocenter based on the calibrated IR coordinate system. Daily calibration removes the system’s sensitivity to small shifts in position of the ceiling mounted, flat panel detectors or IR cameras.

Statistical analysis

In this study, all shifts indicated in the imageguided ExacTrac systems were considered as displacements between the planned treatment isocenter in the phantom or patients and the radiation isocenter of the linear accelerator. The setup errors of the 40 sets of phantom and 225 patients were analyzed using SPSS 19.0 (SPSS Inc., Chicago, IL, USA) and Origin 7.0 (Origin Lab Corparation, Northampton, MA01060 USA) software. The root mean square (RMS) and standard deviation (SD) of the residual setup errors in the LR, SI, and AP translational directions, and rotational variations: pitch, roll, and yaw were calculated.

Images acquisition and registration

At our institution, all treatments of patients are performed using the Trilogy linear accelerator system (Varian Medical Systems, Inc., Palo Alto, USA) used in the study, which was equipped with the ExacTrac system from Brainlab (BrainLABAG, Feldkirchen, Germany). ExacTrac system mainly consists of (1) an infrared (IR)based optical positioning system which is used for initial patient setup and precise control of couch movement with a robotic couch, (2) two floormounted kV Xray tubes which projects medial, anterior, and inferior obliquely into two corresponding flat panel detectors mounted on the ceiling, (3) a radiographic kV Xray imaging system (Xray 6D) for position verification and readjustment based on the internal anatomy or implanted fiducial markers. The X-ray tubes have variable energy (40 kV-150 kV), current (10 mA-320 mA), and time (2 ms-6300 ms) settings for a range of contrast and brightness. The flat panel detectors are 512 x 512 pixels with an active area of 20 cm x 20 cm, which provides a field of view of view of ≈ 13 cm x 13 cm at isocenter with an image pixel size of 0.4 mm◊0.4 mm.

Result

Phantom study

We designed 40 sets of a known range of set-up deviations on the phantoms for repeated measurements. Table 1 lists the range of initial corrections applied to 40 sets of phantom and the corresponding original setup errors with three different VOIs in the LR(X), SI(Y), and AP(Z) directions, and rotational variations: pitch, roll, and yaw. Figure 1 shows box and whisker plots of the translational and rotational variations in the lateral, longitudinal, and vertical directions, and of the rotational variations in the pitch, roll, and yaw dimensions with differences among the VOI of Head & Neck (HN), VOI of Head only (H), and VOI of Neck (N) only when used for cranial verification phantom. Residual setup errors with three different selection in VOI of Head & Neck, VOI of Head only, and VOI of Neck only were listed in Table 2. In lateral direction, RMS residual error differences in VOI of Head & Neck, VOI of Head only, and VOI of Neck only were 0.54 ± 0.40mm, 0.57 ± 0.41mm, 0.78 ± .61mm, respectively. While in longitudinal direction, the corresponding values were 0.52 ± 0.43mm, 0.55 ± 0.44mm, 0.51 ± 0.44mm, respectively. For HN vs H only, only vertical was statistical significant ($p < 0.05$). while for HN vs N only, only lateral was statistical significant ($p < 0.05$). For H only vs N only, three translational directions were statistical significant ($p < 0.05$). In addition, the largest rotational RMS seen predominantly in roll were 0.18mm,0.26mm, 0.35mm respectively in roll with three different VOIs. The differences in rotational directions between HN and H only, N only were statistical significant ($p < 0.05$). However, the difference in pitch roll and yaw directions between H only and N only was not significant ($p = 0.397$, $p = 0.239$ and $p = 0.081$ respectively). Figure 2 shows box and whisker plots of the translational variations in the lateral, longitudinal, and vertical directions, and of the rotational variations in the pitch, roll, and yaw dimensions with differences among the VOI of Head & Neck (HN), VOI of Head only (H), and VOI of Neck (N) only when used for cranial verification phantom. The RMS in the translational dimensions was < 0.6 mm for online matching and < 1.10 mm for VOI of Head & Neck (HN) and VOI of Head only (H) offline matching. For VOI of Neck only(N), the RMS in the translational dimensions with was < 0.8 mm. Furthermore, the RMS in the rotational dimensions was < 0.2° for VOI of Head & Neck (HN) and < 0.3° for VOI of Head only (H) offline matching. For VOI of Neck

only (N), the RMS in the rotational dimensions was < 0.4°. The minimum setup errors were observed when VOI Head & Neck (HN) was selected.

Patient study

Figures 3,4,5 show box and whisker plots of the translational variations in the lateral, longitudinal, and vertical directions, and of the rotational variations in the pitch, roll, and yaw dimensions with differences among the VOI of Head & Neck (HN), VOI of Head only (H), and VOI of Neck (N) only when used for cranial, neck, head & neck cancer patients respectively. For 75 cranial patients, the RMS of differences in all six directions with different selection of VOIs (H only and H&N) were not statistical significant ($p > 0.05$). For 75 neck patients, the RMS of differences in translational directions only lateral direction with different selection of VOIs (N only and H&N) was not statistical significant ($p > 0.05$). In the longitudinal and vertical translational directions, the RMS were statistical significant ($p < 0.05$). In rotational directions, the RMS were statistical significant ($p < 0.05$) in pitch and roll directions. However, in yaw direction the RMS was not statistical significant ($p > 0.05$). For 75 head&neck cancer patients, the RMS of differences in vertical translational direction and pitch and yaw rotational directions with different selection of VOIs (PTV only and H&N) were statistical significant ($p < 0.05$). Other directions were not statistical significant ($p > 0.05$).

Discussion

The popularity of image guided radiation therapy (IGRT) has boosted in recent years. IGRT utilizes a variety of imaging techniques, which are employed immediately preceding to treatment to confirm the patient's position [15–17]. IGRT systems usually used are able to be divided into two groups, including CT-based IGRT and planar-image-based IGRT. Most patients perform radiotherapy were fixed with the use of a removable, non-invasive immobilizing frame (e.g. thermo-plastic mask or occipital pad with bite-block) [18]. For the reason that the frame must be repositioned at each treatment this process lends itself to additional inter-fraction setup uncertainty as a result of the combined effects of head position adjust within the mask in the middle of treatments and daily setup error. Se An Oh, et al (2016) [19] who evaluated the setup uncertainties for brain sites when using BrainLAB's ExacTrac X-ray 6D system for daily pretreatment to determine the optimal planning target volume (PTV) margin. The random errors (σ) were 0.31, 0.46, and 0.54 mm in the lateral, longitudinal, and vertical rotational dimensions, respectively, and 0.28°, 0.24°, and 0.31° in the pitch, roll, and yaw rotational dimensions, respectively.

One feasible solution to improving setup accuracy for stereotactic treatments is image guidance. It is especially true when delivering fractionated IMRT with a non-invasive immobilization system as the innate setup uncertainties. The immobilized patient is setup on the treatment couch and the head ring is mounted to the treatment couch and adjusted so that the planned isocenter is coincident with the linac isocenter. As soon as a setup according to bony anatomy in head and neck cancer is used [20–22], large intra- and inter- fractional tumor position change can be observed at the daily treatment fractions. To put across these geometrical uncertainties in the lack of sufficient correction approaches, the usage of

considerable safety margins is essential. While, these large margins expose adjacent organs to increased radiation doses, which could increase poisonousness and hinder the use of dose increase. If “exact” alignment exist, the two images should be the same in the field of the position of bony anatomy, air cavities, and any internal markers. In order to accomplish the case of optimum alignment the doctors can choose the Automatic 6D Image Fusion feature which uses a mutual information image fusion algorithm to get the optimum match of the bony anatomy between each X-ray image and its corresponding DRR projection over the set of probable translations and rotations from true isocenter, therefore indicating the current patient alignment error. The CT data is used to find the best match by variable projection (i.e. translation from isocentric and rotation around isocentric) and by iteration and maximizing similarity measures (edge detection). Vania Tacher, et al. [23] who compare three types of three-dimensional CBCT-based imaging guidance modalities in a phantom study: image fusion with fluoroscopy (IF), electromagnetic navigation (EMN) and the association of both technologies (CEMNIF) found that efficacy and accuracy of puncture for acute angle access targets with EMN, IF or CEMNIF were similar. EMNIF is more precise for large angle access targets at the cost of a slightly higher procedure time and radiation exposure. It would be interesting to analyze the integrity and constraints of VOI positioning within a practical structure. All these efforts have been concentrated on improving the technology and showing the image quality and dosimetric effects of the VOI selection method. These concerned utilizing comparatively simple phantoms, i.e. cylindrical water phantom with a tissue equivalent insert. Nevertheless, the setting of VOI within a complicated geometry was not a central point. The methods established in this paper show the potential for better image quality with decreased surrounding dose for patients. Yet, there exist several opportunities that may be explored further. The major drawback of the VOI approach used in the paper is that all information outside the VOI is unused in the course of reconstruction. The next progress of this work could be to employ modulation of the field.

Conclusion

The registration accuracy was examined by Extrac cranial verification phantom and patients with varying VOI and to assess. We can conclude that image registration using larger VOI is helpful to improve the registration accuracy. One limitation of the present study is that we only evaluated the influences of different VOIs on setup errors in head and neck cancer patients. If we had included treatment of other regions including chest and abdomen pelvic cavity cancer patients especially SBRT patients, ExacTrac setup errors may also have been introduced. Thus, in future work, we plan to evaluate the setup errors in the ExacTrac 6D X-ray when used in treating extracranial regions.

Declarations

Conflict of interests

The authors declare no other conflict of interests.

Acknowledgments

The study was supported in part by the Natural Science Foundation of Chongqing, China (No. cstc2019jscx-msxmX0265). Technology Innovation and Application Development Project of Chongqing (cstccxljrc201910) and the Cultivation Program for Clinical Research Talents of Army Medical University (2018XLC1010).

References

1. Chen X, Liang R, Zhu X. Anti-EGFR therapies in nasopharyngeal carcinoma. Biomed Pharmacother, **131**,110649 (2020).
2. Wang S, Claret FX, Wu W. MicroRNAs as Therapeutic Targets in Nasopharyngeal Carcinoma. Front Oncol, **9**,756 (2019).
3. Liang ZG. et al. Comparison of radiomics tools for image analyses and clinical prediction in nasopharyngeal carcinoma. Br J Radiol, **92**(**1102**), 20190271 (2019).
4. Wu S. et al. Analysis of intensity-modulated radiotherapy for patients with nasopharyngeal carcinoma. Medicine (Baltimore), **99**(**30**), e21325 (2020).
5. Ibrahim MS, Attalla EM, El Naggar M, Elshemey WM. Is 9-field IMRT superior to 7-field IMRT in the treatment of nasopharyngeal carcinoma? Indian J Cancer, **57**(**4**), 388–392 (2020).
6. Mnejja W. et al. Quel impact de la RCMI des carcinomes nasopharyngés sur les structures glandulaires? [What is the impact of IMRT of nasopharyngeal carcinomas on glandular structures?]. Cancer Radiother, **24**(**1**), 38–43 (2019).
7. Dai X. et al. Head-and-neck organs-at-risk auto-delineation using dual pyramid networks for CBCT-guided adaptive radiotherapy. Phys Med Biol, **66**(**4**), 045021 (2021).
8. Delishaj D. et al. Set-up errors in head and neck cancer treated with IMRT technique assessed by cone-beam computed tomography: a feasible protocol. Radiat Oncol J, **36**(**1**), 54–62 (2018).
9. Graulieres E, Kubler S, Martin E, Ferrand R. Positioning accuracy of a single-isocenter multiple targets SRS treatment: A comparison between Varian TrueBeam CBCT and Brainlab ExacTrac. Phys Med, **80**, 267–273 (2020).
10. Kang H, Patel R, Roeske JC. Efficient quality assurance method with automated data acquisition of a single phantom setup to determine radiation and imaging isocenter congruence. J Appl Clin Med Phys, **20**(**10**), 127–133 (2019).
11. Oh SA, Park JW, Yea JW, Kim SK. Evaluations of the setup discrepancy between BrainLAB 6D ExacTrac and cone-beam computed tomography used with the imaging guidance system Novalis-Tx for intracranial stereotactic radiosurgery. PLoS One, **12**(**5**), e0177798 (2017).
12. Darvish-Molla S, Spurway AJ, Sattarivand M. Comprehensive characterization of ExacTrac stereoscopic image guidance system using Monte Carlo and Spektr simulations. Phys Med Biol, **65**(**24**), 245029 (2020).
13. Keeling V, Hossain S, Jin H, Algan O, Ahmad S, Ali I. Quantitative evaluation of patient setup uncertainty of stereotactic radiotherapy with the frameless 6D ExacTrac system using statistical

modeling. J Appl Clin Med Phys, **17**(**3**), 111–127 (2016).

14. Zhao LR, Qian JD, Duan XJ, Yang DQ, Zhou YB, Li GH. The clinical feasibility and effect of online ExacTrac 6 degree-of-freedom system for head-and-neck cancer. Digital Medicine, *5*, 119–25 (2019).
15. Luh JY. et al. ACR-ASTRO Practice Parameter for Image-guided Radiation Therapy (IGRT). Am J Clin Oncol, **43**(**7**), 459–68 (2020).
16. Zhao LR. et al. The clinical feasibility and performance of an orthogonal X-ray imaging system for image-guided radiotherapy in nasopharyngeal cancer patients: Comparison with cone-beam CT. Phys Med, **32**(**1**), 266–271 (2016).
17. Kearney M, Coffey M, Leong A. A review of Image Guided Radiation Therapy in head and neck cancer from 2009 – 201 - Best Practice Recommendations for RTTs in the Clinic. Tech Innov Patient Support Radiat Oncol, **14**, 43–50 (2020).
18. Li J. et al. Comparison of Online 6 Degree-of-Freedom Image Registration of Varian TrueBeam Cone-Beam CT and BrainLab ExacTrac X-Ray for Intracranial Radiosurgery. Technol Cancer Res Treat, **16**(**3**), 339–43 (2017).
19. Oh SA, Yea JW, Kang MK, Park JW, Kim SK. Analysis of the Setup Uncertainty and Margin of the Daily ExacTrac 6D Image Guide System for Patients with Brain Tumors. PLoS One, **11**(**3**), e0151709 (2016).
20. Ong CL. et al. Intra-fraction and Inter-fraction analysis of a dedicated immobilization device for intracranial radiation treatment. Radiat Oncol, **15**(**1**), 200 (2020).
21. Hoffmann L. et al. Setup strategies and uncertainties in esophageal radiotherapy based on detailed intra- and interfractional tumor motion mapping. Radiother Oncol, **136**,161–168 (2019).
22. Lu L. et al. Intra- and inter-fractional liver and lung tumor motions treated with SBRT under active breathing control. J Appl Clin Med Phys, **19**(**1**), 39–45 (2018).
23. Tacher V. et al. CBCT-Based Image Guidance for Percutaneous Access: Electromagnetic Navigation Versus 3D Image Fusion with Fluoroscopy Versus Combination of Both Technologies-A Phantom Study. Cardiovasc Intervent Radiol, **43**(**3**), 495–504 (2020).

Tables

Table 1 Range of initial corrections applied to the phantom

Serial Number	Initial Coordianates			Registration Error																	
	Translation(mm)			Head&Neck						Head only						Neck only					
				Translation(mm)			Rotation(°)			Translation(mm)			Rotation(°)			Translation(mm)			Rotation(°)		
	X	Y	Z	A_X	A_Y	A_Z	A_P	A_R	A_J	H_X	H_Y	H_Z	H_P	H_R	H_J	N_X	N_Y	N_Z	N_P	N_R	N_J
1	0	0	0	-0.51	0.08	-0.61	-0.06	-0.02	0.36	-0.04	0.12	-0.59	-0.09	0.11	0.03	0.05	0.04	-1.21	-0.36	-0.06	0.67
2	1	1	1	0.34	0.43	0.48	-0.16	-0.05	0.28	0.41	0.55	0.58	0.21	-1.05	0.44	1.14	0.37	-0.24	-0.50	-0.15	0.82
3	2	2	2	0.39	1.47	1.46	-0.14	0.06	0.31	0.42	1.46	1.52	-0.01	-0.78	0.40	0.76	1.52	0.66	-0.44	-0.12	0.56
4	3	3	3	1.40	2.38	2.44	-0.17	0.18	0.27	1.36	2.47	2.46	0.07	-0.24	0.10	1.90	2.36	1.91	-0.36	-0.31	0.59
5	5	5	5	3.28	4.04	4.43	-0.04	0.02	0.33	3.27	4.03	4.44	-0.04	0.36	0.16	3.73	3.91	3.61	-0.46	-0.08	0.61
6	1	0	0	-0.29	-1.23	-0.38	-0.23	-0.16	0.36	-0.13	-1.26	-0.27	-0.10	-0.7	0.55	0.26	-1.30	-0.17	-0.52	-0.24	0.62
7	2	0	0	0.82	-1.19	-0.25	-0.06	-0.10	0.40	0.79	-1.20	-0.27	0.01	-0.66	0.41	1.07	-1.40	-1.24	-0.53	-0.02	0.50
8	3	0	0	1.69	-1.23	-0.32	-0.17	0.06	0.30	1.76	-1.12	-0.29	-0.04	-0.43	0.27	2.44	-1.41	-1.16	-0.60	-0.24	0.74
9	5	0	0	3.41	-1.08	-0.38	-0.06	0.08	0.16	3.46	-1.15	-0.27	0.09	-0.29	0.17	3.86	-1.24	-0.92	-0.4	-0.19	0.52
10	10	0	0	7.90	-1.1	-0.37	-0.07	0.13	0.17	7.92	-1.13	-0.26	0.05	-0.29	0.22	8.39	-1.27	-1.05	-0.47	-0.22	0.55
11	0	1	0	-1.31	0.41	-0.34	-0.15	0.10	0.18	-1.25	0.43	-0.28	-0.06	-0.50	0.26	-0.62	0.41	-0.72	-0.26	-0.02	0.72
12	0	2	0	-1.23	1.50	-0.20	-0.11	0.11	0.37	-1.26	1.56	-0.16	0.167	-0.64	0.33	-0.48	1.53	-1.02	-0.40	-0.10	0.80
13	0	3	0	-1.24	2.84	-0.20	-0.07	0.11	0.35	-1.32	2.93	-0.25	0.03	-0.21	0.08	-0.73	2.89	-0.78	-0.27	0.05	0.62
14	0	5	0	-1.29	4.09	-0.25	-0.18	0.20	0.16	-1.31	4.24	-0.22	0.08	-0.40	0.10	-0.48	4.06	0.96	-0.47	-0.22	0.76
15	0	10	0	-1.25	8.98	-0.28	-0.07	0.08	0.30	-1.28	9.02	-0.32	-0.11	-0.39	0.30	-0.18	8.79	-1.34	-0.62	0.07	0.43
16	0	0	1	-1.37	-0.58	0.48	-0.14	0.04	0.29	-1.32	-0.49	0.43	-0.17	-0.50	0.29	-0.90	-0.54	-0.15	-0.37	-0.05	0.65
17	0	0	2	-1.32	-0.58	1.44	-0.13	-0.01	0.35	-1.30	-0.64	1.51	0.10	-0.42	0.19	-0.59	-0.58	0.74	-0.42	-0.21	0.79
18	0	0	3	-1.41	-0.65	2.51	-0.14	0.05	0.20	-1.38	-0.56	2.48	0.02	-0.32	0.23	-0.97	-0.71	1.78	-0.46	0.06	0.57
19	0	0	5	-1.32	-0.55	4.36	-0.07	0.12	0.32	-1.44	0.53	4.43	0.03	-0.41	0.10	-0.55	-0.71	3.25	-0.67	-0.26	0.77
20	0	0	10	-1.33	0.56	9.25	-0.11	0.19	0.43	-1.28	-0.46	9.18	-0.04	-0.31	0.23	-0.76	-0.59	9.25	-0.46	0.19	0.70
21	0	0	0	-0.03	-0.19	-1.19	-0.22	0.13	0.67	-0.11	-0.14	-1.26	-0.20	-0.33	0.55	0.76	-0.33	-2.62	-0.94	0.42	1.20

Table 2. Residual setup errors and differences among the VOI of Head & Neck, VOI of Head only, and VOI of Neck only when used for head phantom (N = 40)

Number N=40 n=117	Directions	Different VOI						VOI of A vs H only			VOI of A vs N only			VOI of H only vs N only		
		VOI of Head&Neck		VOI of Head only		VOI of Neck only		Difference		p-Value	Difference		p-Value	Difference		p-Value
		RMS	SD	RMS	SD	RMS	SD	RMS	SD		RMS	SD		RMS	SD	
	Translational(mm)															
	Lateral(x-axis)	0.54	0.40	0.57	0.41	0.78	0.61	0.03	0.31	0.609	0.24	0.28	0.000[a]	0.21	0.41	0.003[a]
	Longitudinal(y-axis)	0.52	0.43	0.55	0.44	0.51	0.44	0.03	0.09	0.052	0.01	0.07	0.331	0.04	0.10	0.017[a]
	Vertical(z-axis)	0.34	0.29	0.56	0.45	0.36	0.21	0.22	0.45	0.004[a]	0.03	0.23	0.469	0.19	0.39	0.004[a]
	Rotational(°)															
	Pitch	0.10	0.07	0.21	0.14	0.19	0.12	0.12	0.15	0.000[a]	0.10	0.11	0.000[a]	0.02	0.16	0.397
	Roll	0.18	0.12	0.26	0.21	0.35	0.28	0.08	0.18	0.005[a]	0.17	0.35	0.006[a]	0.08	0.43	0.239
	Yaw	0.09	0.08	0.22	0.18	0.15	0.13	0.13	0.17	0.000[a]	0.06	0.16	0.038[a]	0.07	0.26	0.081

Abbreviation: N=number of scans of phantom; n=number of registrations with different VOI. A: all CT scan range, H: VOI for head only, N: VOI for neck only, [a]p<0.05.

Figures

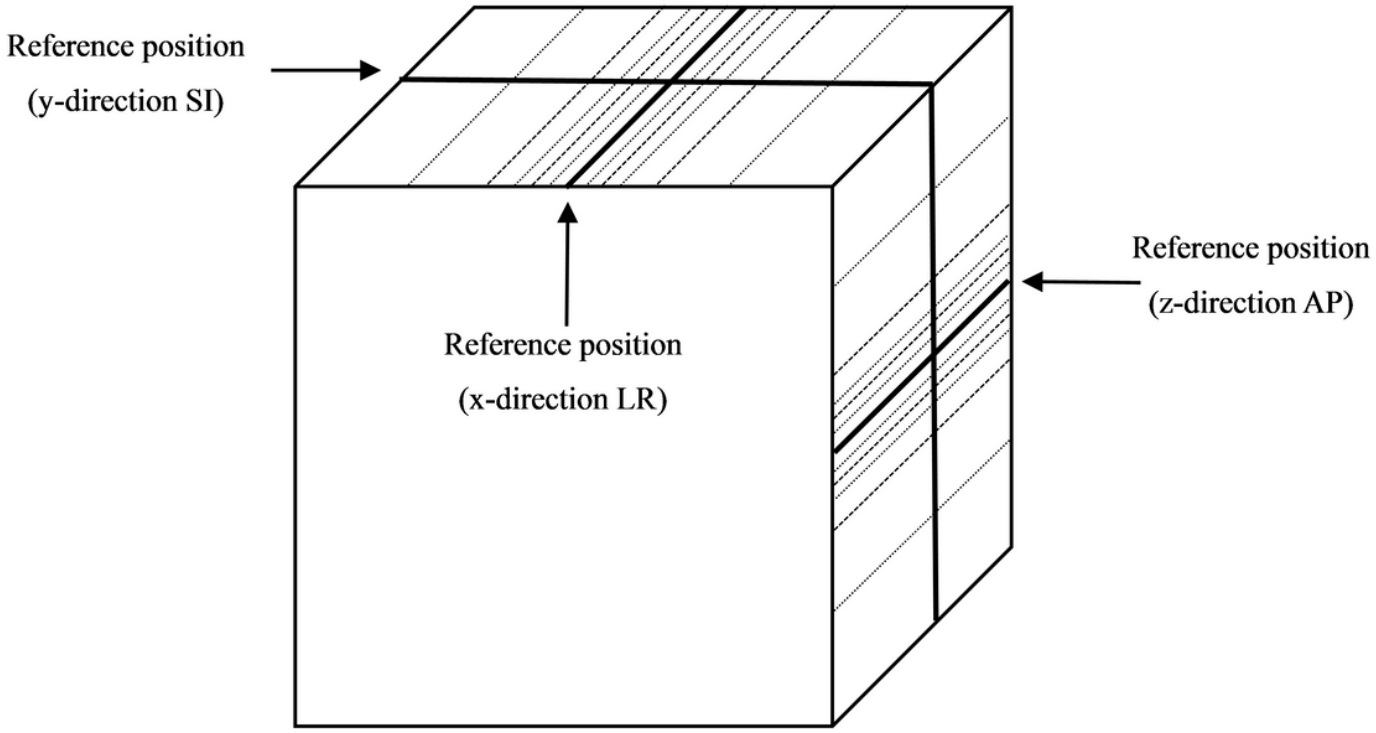

Figure 1

Diagram showing the translational deviation lines in X, Y and Z directions marked on the phantom (not to scale).

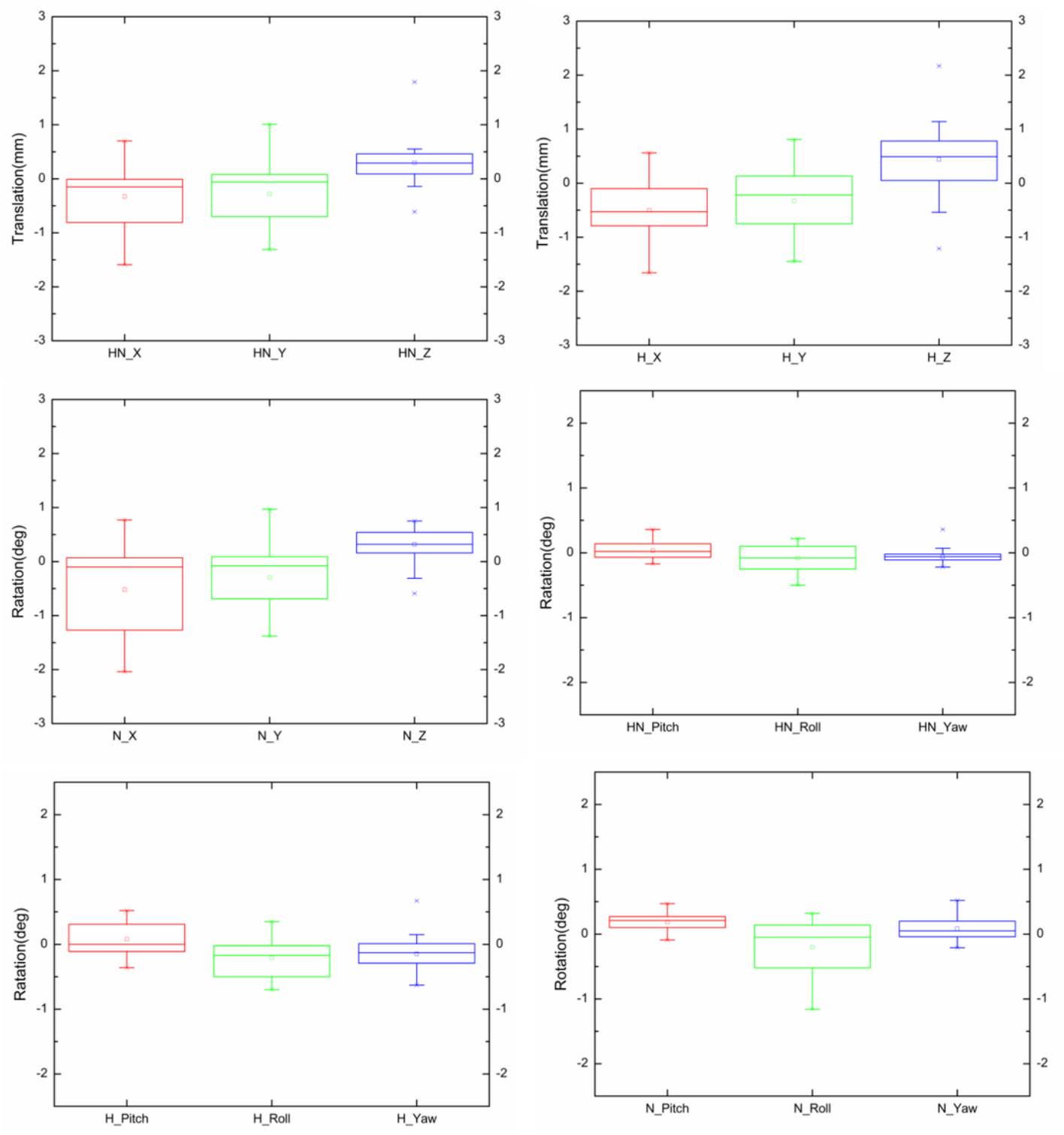

Figure 2

Box and whisker plots of the translational and rotational variations in the latera (X-axis), longitudinal (Y-axis), and vertical (Z-axis) directions and of the rotational variations in the pitch, roll, and yaw dimensions with differences among the VOI of Head & Neck (HN), VOI of Head only (H), and VOI of Neck (N) only when used for cranial verification phantom.

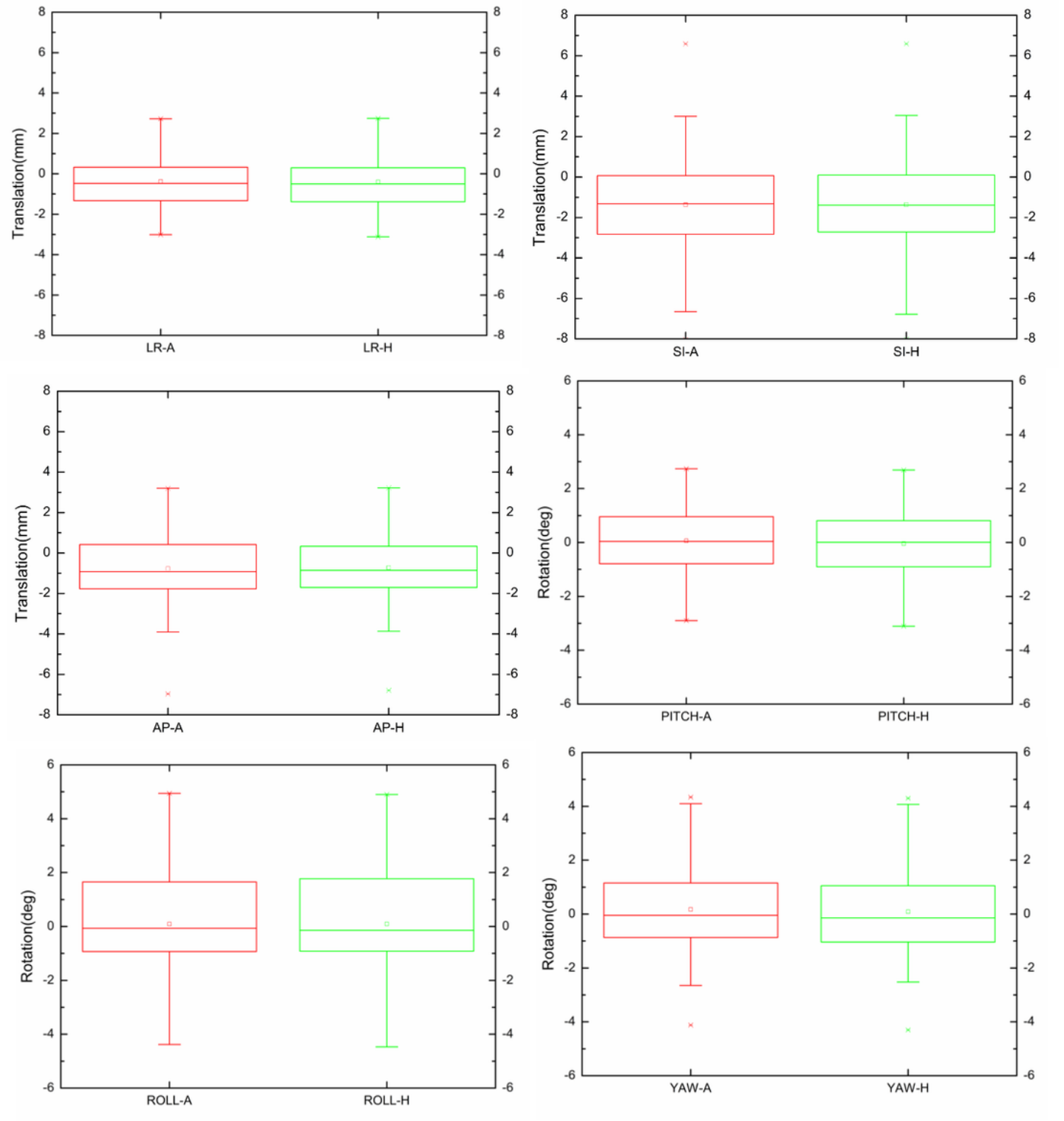

Figure 3

Box and whisker plots of the translational variations in the LR (X-axis), SI (Y-axis), and AP (Z-axis) directions with differences among the VOI of whole CT range (A),, VOI of Head only (H) only when used for head cancer patient.

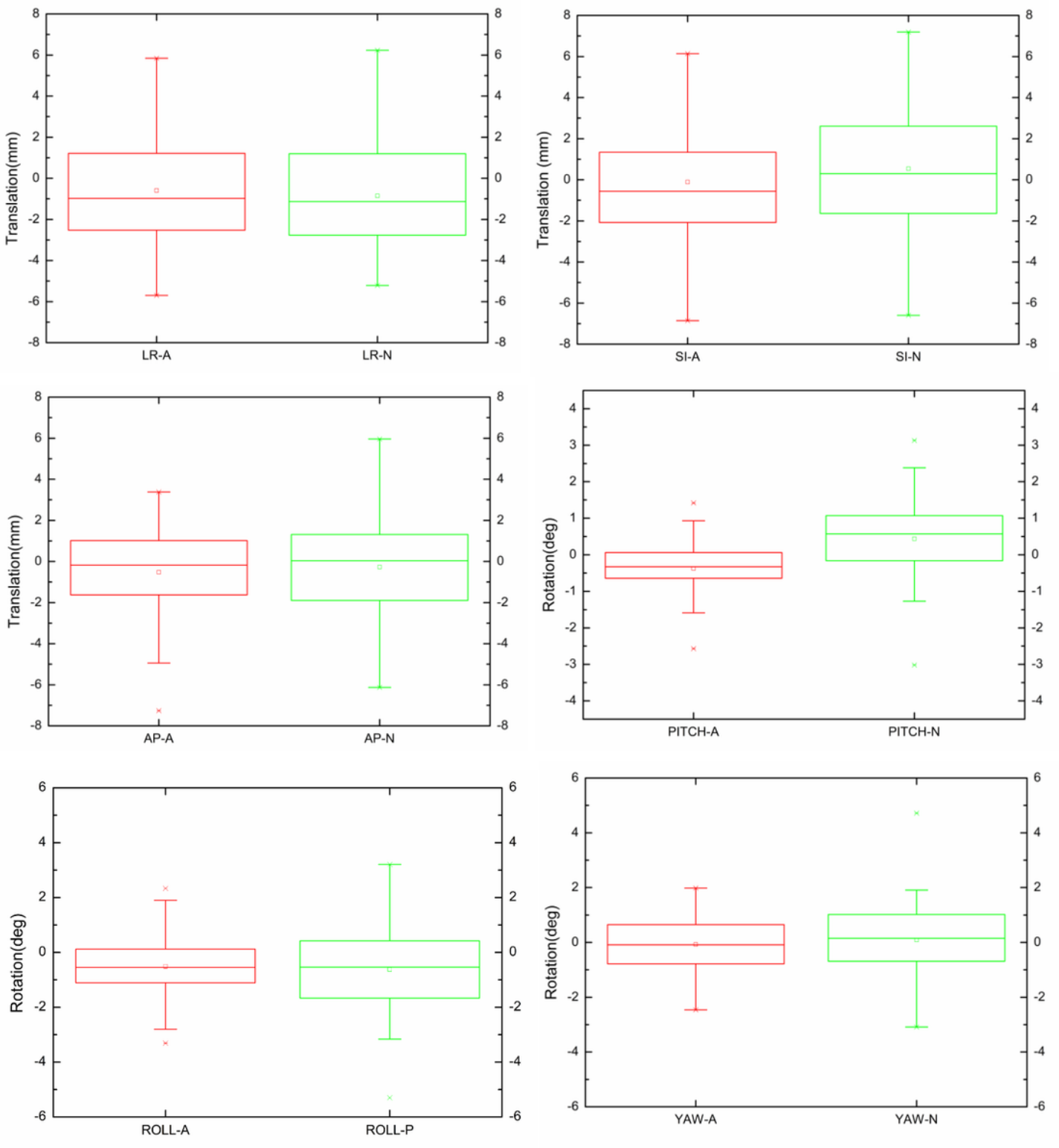

Figure 4

Box and whisker plots of the translational variations in the LR (X-axis), SI (Y-axis), and AP (Z-axis) directions with differences among the VOI of whole CT range (A), and VOI of Neck (N) only when used for neck cancer patient.

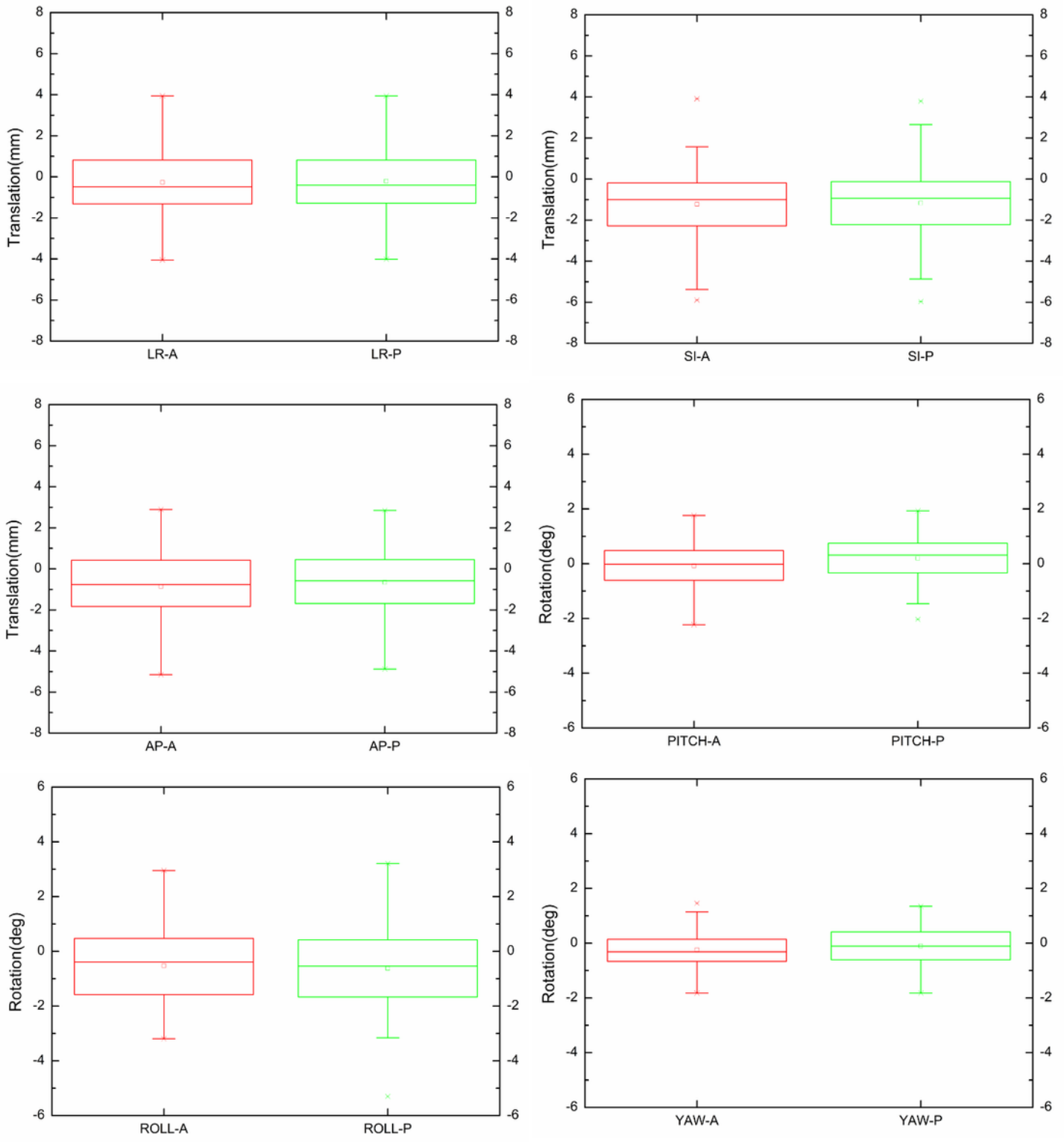

Figure 5

Box and whisker plots of the translational variations in the LR (X-axis), SI (Y-axis), and AP (Z-axis) directions with differences among the VOI of whole CT range (A), VOI of PTV only (P) when used for Head & Neck patient.